ISSN: 0973-3469, Vol.16, No.(2) 2019, Pg. 164-173

Material Science Research India

www.materialsciencejournal.org

# Application of Novel Clay Composite Adsorbent for Fluoride Removal

**LECHISA DABA GIDI, ENYEW AMARE ZEREFFA*, H C ANANDA MURTHY and BUZUAYEHU ABEBE**

Department of Applied Chemistry, School of Applied Natural Science, Adama Science and Technology University, P O Box 1888, Adama, Ethiopia.

**Abstract**

A novel cost-effective, eco-friendly clay composite adsorbent was developed towards fluoride remediation. Clay, Grog, Bone char, and Sawdust were dry mixed within volume ratios of (5:1:1:1), (4:2:2:1), and (3:3:3:1), respectively. The powders were mixed again with distilled water, pressed with disc shape; sun dried for three days and fired for one hour in the muffle furnace at 400 °C, 500 °C, and 600 °C. The cooled discs were ground and sieved to obtain nine different composite powdered with particle size less than 1.18 mm. The developed composite adsorbent was characterized using advanced techniques: XRD, SEM, and FT-IR. The adsorption studies showed that among the developed adsorbents, composite with the volume ratio of (3:3:3:1) and optimized at firing temperature of 400 °C exhibited maximum adsorption capacities of 91.6% fluoride removal efficiency. The XRD analysis revealed mixed phases in the composite, and the presence of $OH^-$ functional groups were indicated by FT-IR analysis. The experimental results indicated that the Langmuir model was found to fit better for the removal of fluoride ion and followed pseudo-second-order rate equation. The composite clay material exhibited excellent removal efficiency for the real water samples analyzed.

**Article History**

Received: 27 May 2019
Accepted: 08 June 2019

**Keywords**

Adsorbent;
Bone Char;
Fired Clay Composite;
Fluoride;
Isotherm.

## Introduction

The presence of fluoride beyond the permitted limits is considered detrimental in drinking water. Contamination of drinking water by fluoride, due to its natural presence from dissolution containing rocks, or by man's activities is one that affects human health and wellbeing.[1–4]

Most of the countires in the world have witnessed people falling victims to fluorosis.[5] Ethiopia is one

**CONTACT** Enyew Amare Zereffa enyewama@yahoo.com Department of Applied Chemistry, School of Applied Natural Science, Adama Science and Technology University, P O Box 1888, Adama, Ethiopia.


Doi: http://dx.doi.org/10.13005/msri/160209

among them, where the population suffers from fluorosis,[6] especially along the Rift Valley zone, where the fluoride concentration was recognized to be highest (10 mg/L).[7]

Many techniques were employed in the past for fluoride remediation.[8] Adsorption was found to be the simplest one. Many organic and inorganic based materials have been applied for the removal of fluoride from drinking water such as lignin, zeolites, carbon nano-tubes, bone char, clays, etc.[2] In view of certain disadvantages of adsorbents, there is a scope for development of simple, nontoxic, eco-friendly and effective adsorbent.[9,10]

The present study was aimed to apply modified clay composite materials prepared by using clay, grog, sawdust, and bone char, as a potential adsorbent for defluoridation. These new composite adsorbents were characterized by using advanced techniques: XRD, SEM, and FT-IR. During the batch adsorption experiment the optimization of solution pH, composite dose, the concentration of adsorbate, and time of adsorbate adsorbent contact was optimized. To know the relation between quantity adsorbed and the amount in bulk phase under equilibrium condition, common adsorption isotherms were used.

## Methods

### Preparation of Clay Composite Adsorbent

The naturally occurring material, clay (C) used in the preparation of composite materials was collected form Kechene, Mariam River. Kechene Woreda is located in Addis Ababa administrations of Gullalle sub-city Woreda at $38^0$45'0"E and $9^0$3'30"N. Grog (G) was made by firing clay, and Sawdust (S) which were collected from Addis Ababa Kechene Women's Pottery Cooperation. The Bone char (B) powder, charred with limited oxygen at 350 °C was supplied by Modjo OSHO Fluoride Removal Technology Center. The collected materials were dried in open air by the sun for 7 days, then ground and sieved separately. Then the dry samples were mixed with the ratios of (5:1:1:1), (4:2:2:1) and (3:3:3:1), and coded as $C_5GSB$, $C_4G_2S_2B$, and $C_3G_3S_3B$, respectively, to represent the clay, grog, sawdust and bone char. The powders were mixed with distilled water, sun-dried for 3 days and nine discs, three from each composite powder were pressed and each of them were fired at 400 °C, 500 °C, and 600 °C for one hour. Finally, they were ground and sieved to obtain nine powdered samples of modified clay ceramic materials with particle size 1.18 mm mesh.

### De-Fluoridation

10 mL of DI water and 2 mL of TISAB were added in a 50 mL plastic beaker containing 10 mL of the sample solution. The sample solution was stirred by a magnetic stirrer then the measurement was done by fluoride ion selective electrode. The fluoride adsorption capacities of the prepared modified clay ceramic materials were evaluated by preliminary tests. The efficiency of adsorption by modified clay ceramic materials ($C_5GSB$, $C_4G_2S_2B$, and $C_3G_3S_3B$) was tested based on their ratio of raw materials and firing temperatures. Then one sample with high percent removal efficiency was identified for further investigation.

### Adsorption Procedure

5 g of composite clay ceramic material was mixed with 100 mL of the water sample containing fluoride ion concentration of 3.12 $mgL^{-1}$ collected from Didibsa village around Walenchit town in 300 mL flask for 4 hours. The resulting solution was centrifuged at 400 rpm for 20 minutes and the filtrate was collected. The final fluoride ion concentration measured after 4h, and again after 48h was equal to 1.003 $mgL^{-1}$. No significant reduction in $F^-$ concentration was found for both measurements. So $F^-$ did not react with adsorption vessels which imply that the remained 2.117 $mgL^{-1}$ of $F^-$ was adsorbed by the prepared adsorbent.

## Results and Discussion

### Silicate Analysis for Determination of Major and Minor Oxides

The silicate analysis of the prepared adsorbent ($C_3G_3S_3B$ fired at 400 °C) is presented in Table 1. The composition of the adsorbent is as follows; 51.42% $SiO_2$, 20.32% $Al_2O_3$, 11.6% $Fe_2O_3$ and 9.40% CaO as major oxides. The adsorbent composite clay ceramic material contains a large amount of silica ($SiO_2$) which indicates that it mainly composed of sandy clay. 11.64% iron oxide ($Fe_2O_3$) in the adsorbent material confirms red clay.

The XRD technique has been one of the most prominent techniques for the identification of the

crystal phase of the adsorbent. Figure 1a show the X-ray diffraction pattern of composite, $C_3G_3S_3B$ material. The major peaks of the composite are associated with those of quartz (2θ = 20, 27 and 50). Other peaks of the raw clay are related to kaolinite (2θ =12 and 24), and muscovite (2θ = 32.02 and 36.15). The peaks of Hydroxyapatite (HA) also appeared at 26°, 30–34° and 40° (2θ). The appearance of multiple broad peaks in the XRD patterns of composite materials may also reveal the presence of the amorphous phase in the composite clay ceramic material.[11]

Figure 2, depicts shift in stretching frequency observed between 3600 and 4000 $cm^{-1}$, 3600 and 3800 $cm^{-1}$ which could beattributed to the involvement of $OH^-$ groups. The adsorption bands at 3430 $cm^{-1}$ show the characteristics of –OH group. FT-IR spectrum revealed that the -OH groups on the adsorbent surface were involved in the sorption of fluoride. The exchange of negative ions through electrostatic attractions is believed to be the prime mechanistic interaction between adsorbent and fluoride. The change in stretching frequency of fluoride-treated composite material confirm the modification in its chemical composition. The peaks appeared at around 500 $cm^{-1}$ most probably due to the presence of metal oxides within the materials.[12,13]

**SEM Micrographs**

The SEM image of composite $C_3G_3S_3B$ fired at 400 °C is given in Figure 3. The image revealed that the adsorbent consists of a large number of tubular structures and porous microstructures which are believed to attribute higher adsorption efficiency to the adsorbent material. It is also concluded that fluorides are adsorbed on the surface regardless of surface irregularities.[14]

**Batch Adsorption Experiment**

**Adsorption Capacities ($C_5GSB$, $C_4G_2S_2B$, and $C_3G_3S_3B$)**

The adsorption capacities and efficiency of the adsorbents were discussed based on values given in Table 2. The efficiency of $F^-$ binding to the composite clay ceramic materials was observed to vary with the firing temperatures and mixture components. At all firing temperatures, the highest fluoride removal capacity from the drinking water was exhibited by $C_3G_3S_3B$ which was fired at 400 °C. As suggested by

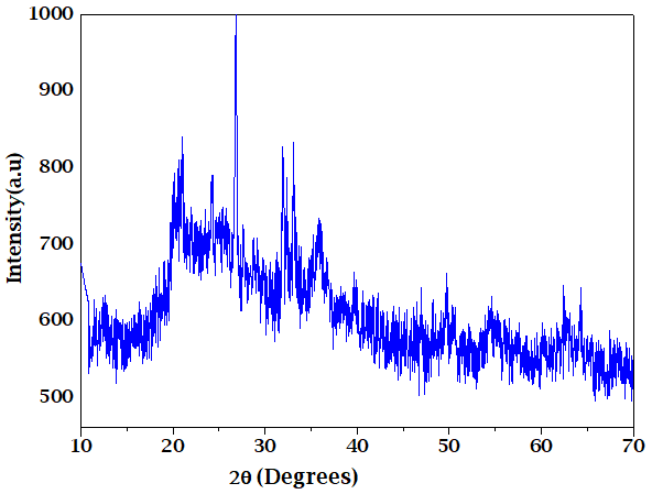


**Fig. 1: XRD patterns of composite, C3G3S3B fired at 400 °C**

**Table 1: The results of silicate analysis in percentage**

| Composite | $SiO_2$ | $Al_2O_3$ | $Fe_2O_3$ | CaO | MgO | $Na_2O$ | $K_2O$ | MnO | $P_2O_5$ | $TiO_2$ | $H_2O$ | LOI |
|---|---|---|---|---|---|---|---|---|---|---|---|---|
| $C_3G_3S_3B$ | 51.42 | 20.32 | 11.64 | 9.40 | 1.24 | 1.00 | 0.20 | 0.08 | 2.46 | 0.27 | 0.09 | 0.54 |

Hauge *et al.*,[15] at 400 °C firing temperature the clay contains more $OH^-$ functional groups and became strong due to the presence of grog in the mixture. During the thermal treatment the sawdust may be converted to charcoal, then to ash, containing oxides of Si, Al, Fe, Ti, Ca, $MgSO_3$ and alkalis along with mixed oxides, as a consequence, its fluoride removal capacity was found to increase, due to the increased surface area to volume ratio.[16] Also as suggested by Shahid *et al.*,[17] for pure bone char 350 °C firing temperature is the optimum for fluoride removal capacity through ion exchange.

**Effect of pH on $C_3G_3S_3B$-400**

Figure 4a presents the influence of pH on $F^-$ adsorption capacity of clay adsorbent. The experiments were conducted for the selected adsorbent at seven different pH values,namely, 2, 3, 4, 5 6, 7 and 8 by keeping the other factors constant (dose: 5 $gL^{-1}$, contact time 4 h and initial fluoride concentration, Co: 5 m $gL^{-1}$). A superior adsorption capacity has been obsereved at highly acidic medium (low pH) which is possibly due to electrostatic attractions resulting in effective defluoridation. It is also reported that positive charges on clay components were found to increase with lowering of pH, thus enhancing the efficiency of defluoridation process.[18] On the other side, decreased adsorption capacity on moving to alkaline pH is because of repressive interaction between $F^-$ and $OH^-$.[19]

At a pH value of 3, highest fluoride adsorption of 91.6% was observed. According to the WHO guideline drinking water with a neutral pH value of 7.0 to 8.5 was desirable for adsorbents to remove fluoride ion.[20] In WHO range desirable conditions, pH = 7.03, the prepared composite material can remove 73% fluoride ion from drinking water. A significant reduction in $F^-$ adsorption at alkaline pH can be attributed to competitive adsorption by $OH^-$ ions.[21]

**Effect of Equilibration Time**

The influence of contact time between the adsorbent and fluoride ions on the adsorption capacity is presented in Figure 4b. In this case, the equilibrium was attained after 4 hours. The sorption percentage increased from 55.4 % at a 1st hour to 72.8 % at the 4th hour. Significant rise in adsorption rate is possibly due to the availability of vacant adsorption sites in the presence of higher fluoride concentration gradient. Afterward, the $F^-$ adsorption rate was found to decrease due to limited availability of vacant adsorption sites and no more binding of fluoride ion occurred beyond saturation. Further, the achievement of the highest binding capacity within 4 hours proposes that a minimum contact time that was adequate enough for defluoridation. The adsorption by adsorbent reached equilibrium at 4h, and 72.8% of fluoride ion was adsorbed, later no change was observed.

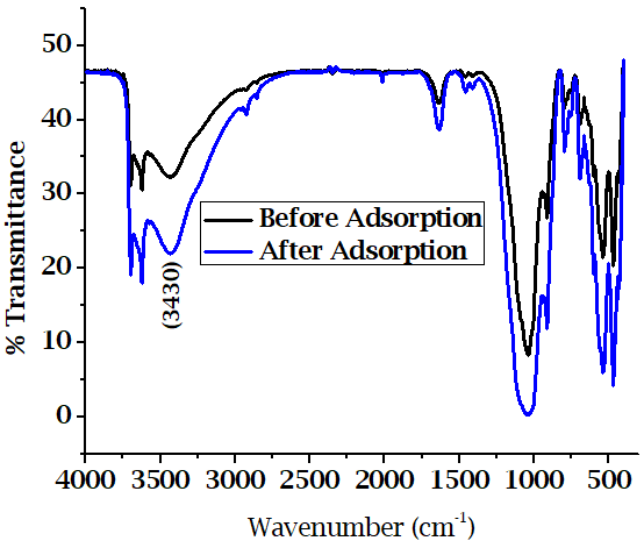


**Fig. 2: IR spectrum of composite, C3G3S3B fired at 400 °C.**

**Effect of Adsorbent Dose**

The experimental result shows that all the composite materials exhibited decreased adsorption capacity and increased adsorption efficiency with increased adsorbent dosage (Figure 4c). It seems that increasing fluoride removal efficiency was found to vary with availability of $F^-$ binding sites. The decrease in capacity is due to the depletion of fluoride in the solution with increasing dose of an adsorbent. Also when the dose is smaller, the number of fluoride ions is significantly higher than that of adsorption sites.[22]

As it was observed on Figure 4c, fluoride removal efficiency was found to increase from 37.6 % to 85% as the adsorbent dose rise from 2.5 g to 10 g (2.5, 5, 7.5, and 10 g). The dose of adsorbent became higher and overlapping of active sites reduced the removal efficiency. This dose of 10 g is believed to be sufficient for defluoridation to the desired standard in dirking water (below 1.5 $mgL^{-1}$).

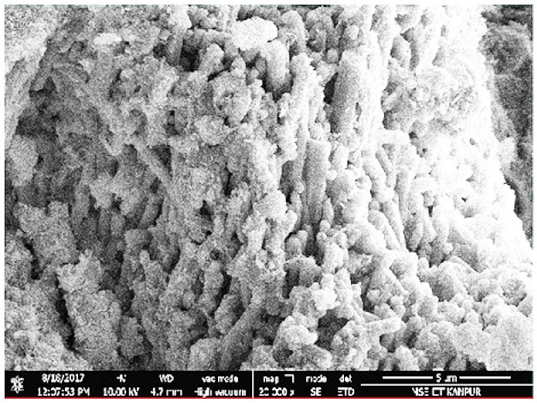

**Fig. 3: SEM image of composite, $C_3G_3S_3B$ fired at 400 °C.**

**Effect of Initial Fluoride Concentration**

For a fixed dose of adsorbent, the fluoride removal capacity (Figure 4d) was found to increase with initial concentration, due to increased diffusion of fluoride to adsorption sites and utilization of less accessible sites on the adsorbent. This indicates the possibility of the formation of multilayer of fluoride ion at the pore volume and interface of the adsorbent.[23]

**Application $C_3G_3S_3B$-400 Adsorbent to the Real Water Samples**

The adsorption process was done by taking all optimized parameters (i.e. the temperature of 24 ± 2 °C, the rotation speed of 400 rpm for 10 min, the contact time of 4h, adsorbent dose = 5 g, at optimized pH of the real water sample = 7.03). Real samples of water were collected from Rift Valley regions of Ethiopia (Oromia region East Showa district, Welachit town around Didibsa, and Maki town around Sarity). Ground water with fluoride ion concentrations of 3.12±0.03 $mgL^{-1}$ and 10.5 ± 0.01$mgL^{-1}$, respectively collected which are more than the permissible limit of WHO. After adsorption,

**Table 2: Adsorption capacity and percent of adsorption of $C_5GSB$, $C_4G_2S_2B$, and $C_3G_3S_3B$ (fired at temperatures of 400 °C, 500 °C and 600 °C) with (adsorbent dose = 10 g, initial fluoride concentration = 9.12 mgL-1, contact time = 1h, and pH value of the solution = 6.7)**

| Firing Temp. (°C) | Samples | Measured values of Ce(mg/L), | | | Ce (mg/L) (Mean ±SD) | % Adsorption | qe(mg/g) |
|---|---|---|---|---|---|---|---|
| | | $C_e$ 1 | $C_e$ 2 | $C_e$ 3 | | | |
| $C_5GSB400$ | C1 | 0.850 | 0.853 | 0.847 | 0.85 ±0.202 | 90.68 | 0.0827 |
| $C_5GSB$-500 | C2 | 0.701 | 0.690 | 0.702 | 0.70 ± 0.301 | 92.32 | 0.0842 |
| $C_5GSB$-600 | C3 | 0.580 | 0.559 | 0.541 | 0.56 ± 0.131 | 93.86 | 0.0856 |
| $C_4G_2S_2B$-400 | C1 | 1.528 | 1.586 | 1.788 | 1.53 ± 0.184 | 83.22 | 0.0759 |
| $C_4G_2S_2B$-500 | C2 | 0.710 | 0.762 | 0.808 | 0.76± 0.531 | 91.67 | 0.0836 |
| $C_4G_2S_2B$-600 | C3 | 0.678 | 0.480 | 0.581 | 0.58± 0.03 | 93.64 | 0.0854 |
| $C_3G_3S_3B$-400 | C1 | 0.601 | 0.543 | 0.662 | 0.60 ± 0.143 | 93.42 | 0.0854 |
| $C_3G_3S_3B$-500 | C2 | 0.887 | 0.892 | 0.890 | 0.89 ± 0.201 | 90.24 | 0.0823 |
| $C_3G_3S_3B$-600 | C3 | 0.583 | 0.382 | 0.776 | 0.58± 0.18 | 93.64 | 0.0852 |

the fluoride ion concentration of the two different samples was measured and the fluoride ion concentration was decreased by C3G3S3B-400 adsorbent material to (1.003±0.124) $mgL^{-1}$ and (3.040 ± 1.293) $mgL^{-1}$, respectively. The composite clay $C_3G_3S_3B$-400 adsorbent had good removal efficiency for the real water samples tested if the optimized dose of the composite is used.

**Adsorption Kinetics**

In this test PFO, PSO, and IPD models were applied to investigate the kinetics of adsorption. The linear equation of PFO (1) and PSO (PSO) becomes:

$$\log(q_e - q_t) = -(K_1 / 2.303)\, t + \log q_e \quad ...(1)$$

$$t/q_t = t/q_e + 1/K_2\, q_e 2 \quad ...(2)$$

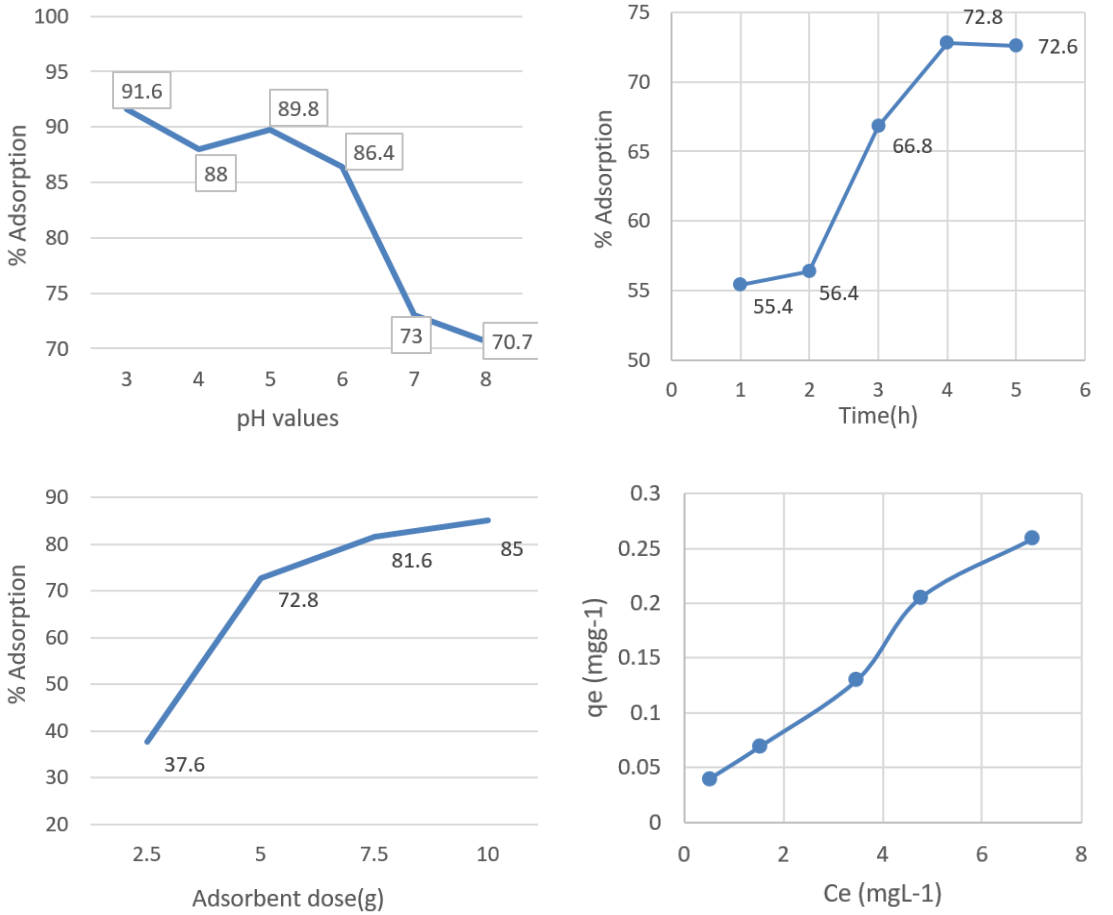


**Fig. 4: a) pH b) Contact period c) Adsorbent dosage d) Initial fluoride concentration for as sytnhesised composite material**

**Table 2: Values of pseudo- first-order, pseudo-second- order, and intra particle diffusion**

| | Pseudo- first-order | | | Pseudo-second- order | | | Intra-particle diffusion | | |
|---|---|---|---|---|---|---|---|---|---|
| $C_o(mgL^{-1})$ | $q_e$(calc.) | $K_1$ | $R^2$ | $q_e$(calc.) | $K_2$ | $R_2$ | $k_i$ | C | $R^2$ |
| 5.0 | 3.47x10-3 | 13.2 | -0.169 | 0.0742 | 52.6 | 0.986 | 0.0164 | 0.0372 | 0.896 |

Where,
$q_e$ and $q_t$ = the amount of fluoride ion adsorbed at equilibrium time and any time, ($mgg^{-1}$), respectively
K1 ($min^{-1}$) and $K_2$ ($gm^{-1}g$ min.) is the rate constant of PFO and PSO, respectively.

As shown on Figure 5 and Table 3 $R^2$ values of PSO (Figure 5b) were found to be higher than those for PFO (Figure 5a,b). This further suggests that the adsorption process proceeds by chemisorption.

To investigate the rate-limiting of the $F^-$ adsorption onto modified fired clay material, the possible contribution of IPD on fluoride adsorption process was tried by using Weber-Morris model.[19]

$$q_t = k_i t^{1/2} + C \quad ...(3)$$

Where,
$q_t$ = amount of fluoride adsorbed at time t ($mgg^{-1}$),
$k_i$ = intra-particle diffusion rate constant ($mgg^{-1}.h^{1/2}$)

The magnitude of the intercept, C is a measure of a thickness of the adsorbed layer. If a linear plot qt versus $t^{1/2}$ passes through the origin, then IPD is the sole rate determining.[12] But as shown in Figure 4c,

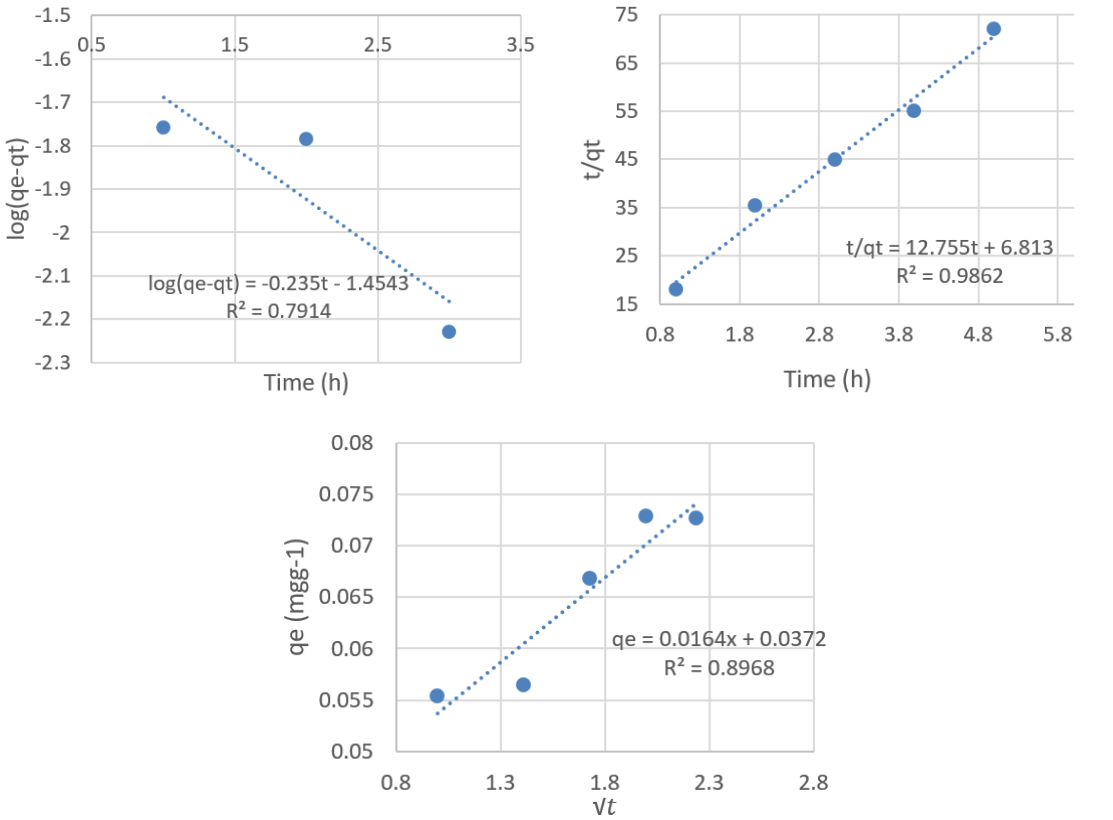


**Fig. 5: a) Plot of pseudo-second-order b) Plot of pseudo-second-order c) Plot of intra-particle diffusion kinetic modeling**

**Table 3: Values of pseudo- first-order, pseudo-second- order, and intra particle diffusion**

| | Pseudo- first-order | | | Pseudo-second- order | | | Intra- particle diffusion | | |
|---|---|---|---|---|---|---|---|---|---|
| $C_o(mgL^{-1})$ | $q_e$(calc.) | $K_1$ | $R^2$ | $q_e$(calc.) | $K_2$ | $R^2$ | $k_i$ | C | $R^2$ |
| 5.0 | $3.47x10^{-3}$ | 13.2 | -0.169 | 0.0742 | 52.6 | 0.986 | 0.0164 | 0.0372 | 0.896 |

the linear plot was not passing through the origin, which indicating complex mechanism for the $F^-$ adsorption on this adsorbent.

The rate determining step was found to be influenced by surface adsorption as well as intra-particle diffusion. This intraparticle diffusion confirms that adsorption of fluoride ion on this adsorbent was a multi-step process.[24]

**Adsorption Isotherms**

Many studies show, adsorption isotherm curves for $F^-$ adsorption onto metal oxide surfaces can be well represented by Langmuir model. Langmuir derived the model based on some reasonable assumptions like uniform adsorption surface, monolayer adsorption, and constant temperature and also assumed equal rates of adsorption and desorption at equilibrium. Using the Linear forms of the Langmuir equation:

$$C_e/q_e = C_e/Q_e + 1/(bQ\text{-}e) \quad ...(4)$$

Where,

$q_e$ = amount of fluoride adsorbed per unit mass of adsorbent (mg/g),

$C_e$ = equilibrium concentration of the adsorbate ($mgL^{-1}$)

$Q_e$ = maximum adsorption capacity

b = energy of adsorption.

Langmuir parameters $Q_e$ and b are determined from the slope and intercept of the linear plot.

The prime characteristics of the Langmuir isotherm can be expressed by a dimensionless s parameter, $R_L$ which is given as:

$$R_L = 1/(1 + bC_o) \quad ...(5)$$

Where,

$C_o$ = Initial concentration of the adsorbate in the solution,

b = Langmuir's adsorption constant (L/mg).

The value of $R_L$ signifies the type of isotherm; If, ($0<R_L<1$) then favourable; If ($R_L>1$) then unfavourable; If ($R_L= 0$) the process is irreversible.

$R_L$ values at different adsorbate initial concentration

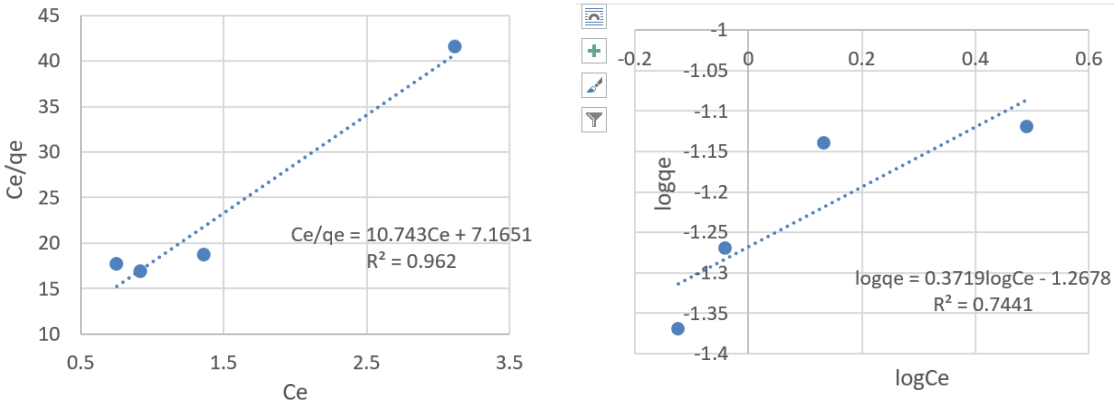


**Fig. 6: Plot of a) Langmuir and b) Freundlich adsorption isotherms model**

**Table 4: Results of the Langmuir and Freundlich adsorption isotherms studies for adsorption of fluoride ion on modified clay composite materials**

| | Langmuir isotherm parameters | | | Freundlich adsorption isotherm | | | |
|---|---|---|---|---|---|---|---|
| Adsorbent | $Q_e$ ($mg.g^{-1}$) | b ($L.mg^{-1}$) | $R^2$ | $R_L$ | $K_f$ ($mg.g^{-1}$) | 1/n | $R^2$ |
| C3G3S3B-400 | 0.093 | 1.50 | 0.962 | 0.118 | 0.534 | 0.372 | 0.744 |

were calculated (Table 4) to confirm lamgmuir adsorption. The $R_L$ value = 0.118, lies between 0 and 1 which confirms that the process is favorable. The results shown in Figure 6a indicates that all experimental data well fitted to the Langmuir isotherm, and the related correlation coefficient is R2 = 0.962.

Adsorption capacity ($Q_e$ = inverse of the slope of the Langmuir isotherm line) of 0.093 was obtained for modified clay ceramic material ($C_3G_3S_3B$ heat treated at 400 °C). The Freundlich isotherm equation takes into account repulsive interactions between adsorbed solute particles and also account for surface heterogeneities. The logarithm form of Freundlich isotherm is given as follows[25]:

$$\text{Log } q_e = 1/n \log C_e + \log K_f \quad ...(6)$$

Where,

$q_e$ = Amount of fluoride ion adsorbed at equilibrium,
$C_e$ = Concentration of fluoride solution at equilibrium,
$K_f$ = equilibrium constant
1/n = type of isotherm.

1/n value found between 0 and 1, (0<1/n <1), i.e. (1/n = 0.372) for this study. Freundlich isotherm is also favorable. The value of correlation coefficients ($R^2$ = 0.962) for Langmuir isotherm is higher in comparison to that obtained for Freundlich isotherm ($R^2$ = 0.744) (Table 4) (Figure 6b). Langmuir isotherm model fits better for adsorption of fluoride ion than Freundlich isotherm on the basis of the experimental study.

## Conclusion

This work involved the study of the preparation, characterization, and application of clay composite materials for defluoridation of drinking water. Clay composite adsorbents were prepared using different ratios of clay, grog, sawdust, and bone char. The developed adsorbents were characterized with XRD, FT-IR, and SEM. The adsorbent with volume ratio 3:3:3:1 of clay, grog, sawdust, and bone char mixed, pressed and fired at 400 °C was found to have 91.6% and 73% fluoride removal efficiency at pH 3.0 and 7.03 respectively. The main methods used in defluoridation from aqueous solutions with the developed composite are ion exchange and adsorption techniques. Langmuir and Freundlich models were employed for the adsorption studies. Langmuir isotherm model was found to fit better for adsorption of fluoride ion than Freundlich isotherm on the basis of the experimental study.The kinetic adsorption study proves that both the adsorption-reaction (PSO) and adsorption-diffusion (IPD) models participated in the adsorption mechanism.

## Acknowledgments and Funding Source

Authors are thankful to the Adama Science and Technology University Research Office for the financial support and OSHO Fluoride Removal Technology Center for providing laboratory facilities.

## Conflict of interest

The authors declare no conflicts of interest.

## References

1. Tripathy S.S., Bersillon J.L. & Gopal K. Removal of fluoride from drinking water by adsorption onto alum-impregnated activated alumina. *Sep. Purif. Technol*. 50, 310–317 (2006).
2. Mohapatra M., Anand S., Mishra B.K., Giles D.E. & Singh P. Review of fluoride removal from drinking water. *J. Environ. Manage*. 91, 67–77 (2009).
3. Peng S. , Zeng Q. , Guo Y. , Niu B. , Zhang X. and Hong S. Defluoridation from aqueous solution by chitosan modified natural zeolite. *J. Chem. Technol. Biotechnol.* 88, 1707–1714 (2013).
4. Ravikumar A. Mitigation of Fluoride from Groundwater by Natural Clay as an Adsorbent. *Iran. J. Energy Environ*. 6, 316–322 (2015).
5. Karthikeyan G., Pius A. & Alagumuthu G. Fluoride adsorption studies of montmorillonite clay. *Indian J. Chem. Technol*. 12, 263–272 (2005).
6. Mahramanlioglu M., Kizilcikli I. & Bicer I. Adsorption of fluoride from aqueous solution by acid treated spent bleaching earth. *J. Fluor.*

*Chem*. 115, 41–47 (2002).
7. Pittet D., Allegranzi B. & Boyce J. The World Health Organization Guidelines on Hand Hygiene in Health Care and Their Consensus Recommendations. *Infect. Control Hosp. Epidemiol*. 30, 611–622 (2009).
8. Thole B. Defluoridation kinetics of 200 °c calcined bauxite, gypsum, and magnesite and breakthrough characteristics of their composite filter. *J. Fluor. Chem*. 132, 529–535 (2011).
9. Ugochukwu U.C., Sarkar B., Rusmin R., Manjaiah K.M. & Mukhopadhyay R. Modified clay minerals for environmental applications. Modif. Clay Zeolite Nanocomposite Mater. 113–127 (2018). doi:10.1016/b978-0-12-814617-0.00003-7
10. Abida Kausar, Munawar Iqbal, Anum Javed, Kiran Aftab, Zill-i-Huma Nazli, Haq Nawaz Bhatti, Shazia Nouren. Dyes adsorption using clay and modified clay: A review. *J. Mol. Liq*. 256, 395–407 (2018).
11. Nature P. Structural Transformations of Hydrolysates Obtained from Ti-, Zr-, and Ti, Zr-Solutions Used for Clay Pillaring: Towards Understanding of the Mixed Pillars Nature Krzysztof. *Materials (Basel*). 44, (2019).
12. Abebe B. & Ananda Murthy H.C. Synthesis and Characterization of Ti-Fe Oxide Nanomaterials for Lead Removal. *J. Nanomater*. 2018, 1–10 (2018).
13. Uzarowicz Ł., Skiba S., Skiba M. & Segvic A. B. Clay-Mineral Formation In Soils Developed In The Weathering Zone Of Pyrite-Bearing Schists : A Case Study From The Abandoned Pyrite ´ Ciszowice , Lower Silesia , Sw Poland. *Clays Clay Miner*. 59, 581–594 (2011).
14. Rout T.K., Verma R., Dennis R.V. & Banerjee, S. Study the Removal of Fluoride from Aqueous Medium by Using Nano-Composites. *J. Encapsulation Adsorpt. Sci.* 05, 38–52 (2015).
15. Hauge S., Österberg R., Bjorvatn K. & Selvig K.A. Defluoridation of drinking water with pottery: effect of firing temperature. *Eur. J. Oral Sci*. 102, 329–333 (1994).
16. Goswami D. & Das A.K. Removal of fluoride from drinking water using a modified fly ash adsorbent. *J. Sci. Ind. Res.* (India). 65, 77–79 (2006).
17. Shahid M.K., Kim J.Y. & Choi Y.G. Synthesis of bone char from cattle bones and its application for fluoride removal from the contaminated water. *Groundw. Sustain. Dev*. 8, 324–331 (2019).
18. Obijole O., Gitari M., Ndungu P. & Samie A. Mechanochemically Activated Aluminosilicate Clay Soils and their Application for Defluoridation and Pathogen Removal from Groundwater. *Int. J. Environ. Res. Public Health* 16, 654 (2019).
19. Embiale A., Chandravanshi B.S. & Zewge F. Levels of fluoride in the Ethiopian and imported black tea (camellia sinensis) infusions prepared in tap and fluoride-rich natural waters. *Int. J. Food Eng*. 10, 447–455 (2014).
20. Tor A., Danaoglu N., Arslan G. & Cengeloglu Y. Removal of fluoride from water by using granular red mud: Batch and column studies. *J. Hazard. Mater*. 164, 271–278 (2009).
21. Raichur A. & Jyoti Basu M. Adsorption of fluoride onto mixed rare earth oxides. *Sep. Purif. Technol*. 24, 121–127 (2001).
22. Suganandam K., Paruthimalkalaigan G., Neeraja P. & Pragathiswaran C. Defluoridation of water using bioadsorbents. *Pollut. Res*. 29, 707–711 (2010).
23. Masindi V., Gitari W.M. & Pindihama K.G. Synthesis of cryptocrystalline magnesite/ bentonite clay composite and its application for removal of phosphate from municipal wastewaters. *Environ. Technol*. (United Kingdom) 37, 603–612 (2016).
24. Bhattacharyya K.G. & Sharma A. Azadirachta indica leaf powder as an effective biosorbent for dyes: A case study with aqueous Congo Red solutions. *J. Environ. Manage*. 71, 217–229 (2004).
25. Buzuayehu Abebe and Ananda Murthy H C, Fe-Oxides Nano-Materials: Synthesis, Characterization and lead sorption property. *Journal of Encapsulation and Adsorption Sciences,* 8, 195-209, (2018).